EXPERIMENTAL AND NUMERICAL STUDIES OF FLUIDIZATION IN A CIRCULATING FLUIDIZED BED

Ahmad Hussain[1,*], Farid Nasir Ani[1], Amer Nordin Darus[1], Azeman Mustafa[2],

[1]Faculty of Mechanical Engineering, Universiti Teknologi Malaysia, Skudai 81310, Johor, Malaysia
[2]Faculty of Chemical and Natural Resources Engineering, Universiti Teknologi Malaysia, Skudai 81310, Johor, Malaysia

***Corresponding Author: Phone: +607-5534785, Fax: +607-5566159**
***Email: ahmad@siswa.utm.my**

ABSTRACT

The hydrodynamics of a circulating fluidized bed (CFB) risers is highly complex and is strongly influenced by the distribution of particles, which is governed by the amount of particles, size, form (e.g. spherical or elliptic), density, etc. The CFB riser column has 265 mm (width), 72 mm (depth) cross-section (rectangle) and 2.7 m height. The riser is made up of interchangeable Plexiglas columns. In this study the influence of the amount of particles on the flow pattern in the CFB system is investigated. The particle loading is increased from a dilute to a dense and gas-particle flow is analyzed.

Simulations were done using FLUENT 6.1, a CFD package by Fluent Inc. Palm shell particles and air were used as the solid and gas phases, respectively. The simulations were done using the geometrical configuration of a CFB test rig at the Universiti Teknologi Malaysia (UTM).

The result discusses the variation of velocity contours, along the riser column and in the riser exit geometry. The effect is significant in the upper region of the riser column and the velocity contours are also influenced by the exit geometry. Simulations results predict that the riser exit cause an upstream exit region of increased solid volume fraction. Experimental and computational results are matched to reasonable agreement. Experimental findings have also helped to refine the numerical modeling of multiphase CFB system.

Keywords: CFD, FLUENT, hydrodynamics, multiphase flow, riser exit, velocity contours

INTRODUCTION

Despite their widespread applications of the CFB, much of the development and design of fluidized bed reactors have been empirical in nature. This is due to the complex flow behaviour of gas-solid flow in these systems which makes flow modeling a challenging task.

The fundamental problem encountered in modeling hydrodynamics of fluidized bed is the motion of the two phases of which the interface is unknown and transient, and the interaction is understood only for a limited range of conditions. [1]

Due to the mathematical complexities of the non-linearity of the equations and in defining the interpenetrating and moving phase boundaries make numerical solutions very difficult [2]. Computational fluid dynamics (CFD) is emerging as a very promising new tool in modeling hydrodynamics. While it is now a standard tool for single-phase flows, it is at the development stage for multiphase systems, such as fluidized beds. [3]

Simulations were performed by [4] in fluidized bed with the presence of air and sand using FLUENT 4.56. The research was carried out at various velocities. The performance of the bed was better at higher gas velocities.

Many researchers have simulated three-dimensional two fluids CFD model of gas particle flow in the CFB using the code CFX-4.3. The turbulence was modeled by k-ε turbulence model in the gas phase and a fixed particle viscosity model in the solid phase. This CFD model showed good agreement with the experiment. [5]

A study of gas/particle flow behavior in the riser section of a circulating fluidized bed (CFB) was done using FLUENT 4.4. Fluid Catalytic Cracking (FCC) particles and air were used as the solid and gas phases, respectively. The computational results showed that the inlet and outlet design have significant effects on the overall gas and solid flow patterns and cluster formations in the riser. [6]

CFB USED FOR SIMULATION

Figure 1 shows the schematics of the CFB used for simulation. This CFB is still in the commissioning phase and the experimentation is expected to start soon. This system consists of an air supply device (blower), a distributor of stainless steel, a fast column of Plexiglas and primary and secondary cyclones of steel and a solid feeding system. The riser and its exit are made of Plexiglas to see the flow behaviour and to perform image analysis.

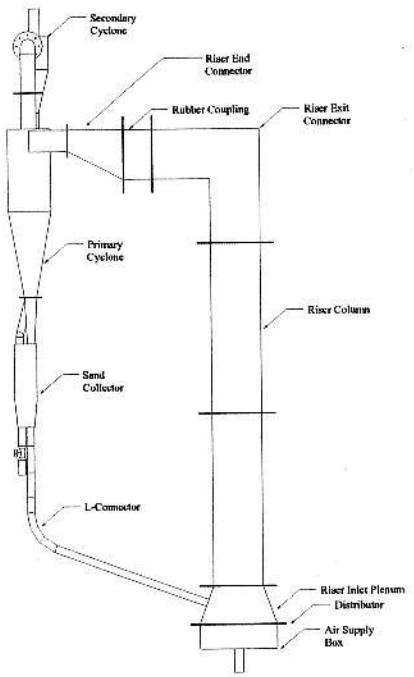

Figure 1: Circulating fluidized test rig at Universiti Teknologi Malaysia

The simulation work described here was done on a riser of rectangular cross-section of 265 (width) x 72 (depth) x 2649 (height) mm^3. The operating parameters were chosen to so give dynamical similarity with a large CFBCs. Simulation was done using FLUENT 6.1, a computational fluid dynamics (CFD) package by Fluent Inc. [7]. Sand particles and air were used as the solid and gas phases, respectively. The parameters used in the simulation work are being summarized in Table 1.

Table 1: Parameters used in simulation work

Parameter	Range of values
Riser dimensions	2649 (L) X 265 (W) mm X 72 (T) mm
Gas velocity	5 m/s
Particle velocity	2 m/s
Properties of air	Density: 1.225 kg m^{-3} Viscosity: 1.79 x 10^{-5} kg/m.s
Properties of particle	Density: 1600 kg m^{-3} Diameter: 100X 10^{-6} m
Height of the particle inlet from distributor	200 mm
Exit Geometries Simulated	Right angle exit, right angle exit with baffle and blind T exit.
Volume fraction of particles	0.03 used as the Algebraic Slip Mixture Model gives good prediction within 10% volume fraction of sand
Granular properties	Particle-particle restitution coefficient is 0.95 Particle-wall restitution coefficient of 0.9
Multiphase model	Eulerian granular multiphase model

RISER EXIT

A wide range of experimental riser exits, which have been reported in the literature. The bend exits shown are characterized by a centerline radius of curvature. Blind T exits are characterized by a roof extension height, a special case is the right angle exit, where extension height is zero. They are most commonly used in industrial CFBCs. These geometries are being shown in Figure 2.

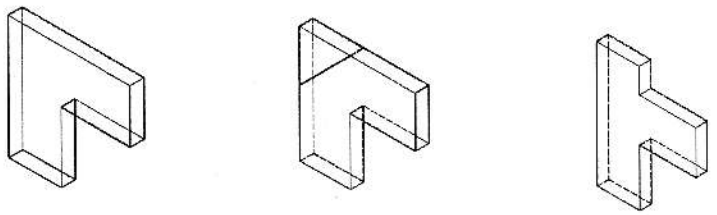

(a) (b) (c)

Figure 2: Riser Exits (a) Right angle exit (b) right angle exit with baffle (c) blind T exit

The findings of [8] & [9] indicate that riser exits can affect the gross-behaviour of a CFB. If more solids accumulate near the riser exit then fewer solids reside in the return leg and therefore the static pressure head in the return leg and consequently M_S, are smaller. The lower rate of solids circulation may cause the solids volume fraction in the riser and connector to be lower. However,

if the solids accumulation near the riser exit extends into these components, the solids volume fraction may be larger. The upstream exit region is generally characterized by a Core/Annulus (C/A) structure, but that the solids mass flux profile may be asymmetric. Some riser exits appear to invoke regions near the riser wall where solids motion is upwards.

The four mechanisms are: inward/outward motion, secondary flow of the first kind, tangential acceleration/deceleration and cavity formation. These mechanisms have shown to influence many of the experimental results. These are being discussed separately below.

a) Inward /outward motion

Owing to their high density, solids in the core region of a riser exit may slip either to the outside or to the inside of the exit, dependent on the relative magnitudes of their inertia and the acceleration due to gravity g. This is being shown in Figure 3. The ratio of solids inertia to gravity may be represented by the following Froude number:

$$Fr_R = \frac{\bar{u}_{st}^2}{gR}$$

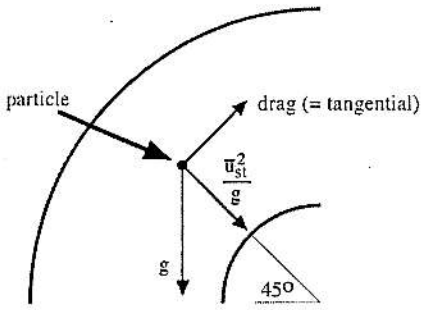

Figure 3: Motion of particle in exit bend

The Froude number Fr_R is dependent on the cross-section average solids velocity near the top of the riser $\bar{u}_{st}$ and on the average radius of curvature R, which is defined by:

$$R = \sqrt{R_{ei}^2 + R_{eo}^2}$$

Here R_{ei} and R_{eo} are the centerline radii of curvature at the inlet and outlet of the riser exit, respectively. The Froude number Fr_R may be expected to be a function of the exit geometry, the superficial gas velocity U_o, and the superficial solids mass flow rate G_s.

b) Secondary flow of the first kind

Bends impose secondary flow of the first kind whereby high momentum fluid in the core moves to the outside of the bend, and slow moving fluid near the wall to the inside of the bend. As a result, the point of maximum velocity lies in the outer half of the bend.

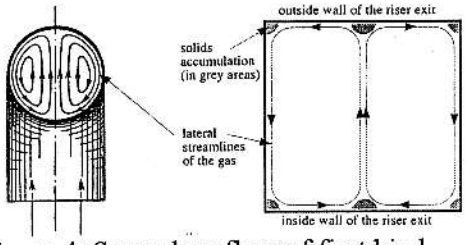

Figure 4: Secondary flow of first kind

A high momentum suspension in the core of a riser exit may invoke similar lateral patterns. Figure 4 shows secondary flow patterns in a bend exit with a square cross-section. It appears that velocity gradients are large near corners and in the middle of the inner and outer wall. Due to their high inertia, solids may accumulate in these areas.

c) Tangential acceleration /deceleration

Tangential acceleration or deceleration of the gas takes place in riser exits with cross-sections that change in size from inlet to outlet. A right angle exit with internal baffle yields acceleration followed by deceleration, a right angle or blind T exit yields deceleration followed by acceleration, and exits with unequal size inlet and outlet impose a net acceleration or deceleration.

Although solids may tend to retain their initial velocity due to their high inertia, they will slow down where the gas decelerates and speed up where the gas accelerates, due to drag between the phases. Since solids entrainment generally increases with the superficial gas velocity, a lower reflux is expected for regions of tangential acceleration and higher reflux for regions of tangential deceleration.

d) Cavity formation

Some riser exits may invoke cavities or regions where solids are disengaged from the main flow. An example is the blind T exit which invokes a cavity in the extension. Solids which enter the extension may hit the roof or, if the extension is sufficiently long, decelerate due to drag from the gas. Consequent build-up of downward momentum may enhance solids return to the riser. If all solids decelerate due to drag, any further extension of the roof may not increase the solids volume fraction in the riser and riser exit.

A small cavity or recirculation eddy may exist in the outer angle of the right angle exit, due to shear from two walls in this area. Cavities may also exist just below inlets of annular plate exits and below inlet baffles.

EULERIAN MULTIPHASE MIXTURE MODEL

The FLUENT modeling is based on the three-dimensional conversation equations for mass, momentum and energy. The differential equations are discretized by the Finite Volume Method and are solved by the SIMPLE algorithm. As a turbulence model, the k-ε was employed; this consists of two transport equations for the turbulent kinetic energy and its dissipation rate. The FLUENT code utilizes an unstructured non-uniform mesh, on which the conservation equations for mass, momentum and energy are discretized. The k-ε model describes the turbulent kinetic energy and its dissipation rate and thus compromises between resolution of turbulent quantities and computational time. The various FLUENT models used in simulations are being tabulated in Table 2.

Table 2: List of FLUENT Models used in simulation

Model	Settings
Space	2D
Time	Steady
Viscous	Standard k-epsilon turbulence model
Wall Treatment	Standard Wall Functions
Multiphase Model	Eulerian Multiphase Model

In the FLUENT computer program that the governing equations were discretized using the finite volume technique. The discretized equations, along with the initial and boundary conditions, were solved to obtain a numerical solution.

The model used for simulating the gas-solid flow is the Eulerian Multiphase Mixture Model (EMMM). The EMMM solves the continuity equation for the mixture, the momentum equation for the mixture, and the volume fraction equation for the secondary phase, as well as an algebraic expression for the relative velocity.

By using the mixture theory approach, the volume of phase q, V_q is defined by

$$V_q = \int_V \alpha_q \, dV$$

and $\sum_{q=1}^{n} \alpha_q = 1$

The effective density of phase q is $\hat{\rho} = \alpha_q \rho_q$

Where ρ_q is the physical density of phase .

Conservative Equations

The general conservation equations from which the solution is obtained by FLUENT are being presented below:

The continuity equation for phase q is

$$\frac{\partial}{\partial t}(\alpha_q \rho_q) + \nabla.(\alpha_q \rho_q \vec{v}_q) = \sum_{p=1}^{n} \dot{m}_{pq}$$

where $\vec{v}_q$ is the velocity of phase q and $\dot{m}_{pq}$ characterizes the mass transfer from the p^{th} to q^{th} phase.

From the mass conservation we can get:

$$\dot{m}_{pq} = - \dot{m}_{qp}$$

and $\dot{m}_{pp} = 0$

Usually, the source term ($\sum_{p=1}^{n} \dot{m}_{pq}$) on the right hand side of equation is zero.

The momentum balance for phase q yields

$$\frac{\partial}{\partial t}(\alpha_q \rho_q \vec{v}_q) + \nabla.(\alpha_q \rho_q \vec{v}_q \vec{v}_q) = -\alpha_q \nabla p +$$
$$\nabla.\bar{\tau}_q + \alpha_q \rho_q \vec{g} + \sum_{p=1}^{n} \left(\vec{R}_{pq} + \dot{m}_{pq} \vec{v}_q\right) +$$
$$\alpha_q \rho_q (\vec{F}_q + \vec{F}_{lift,q} + \vec{F}_{vm,q})$$

Where $\bar{\tau}_q$ is the q^{th} phase stress-strain tensor.

$$\bar{\tau}_q = \alpha_q \mu_q (\nabla \vec{v}_q + \nabla \vec{v}_q^{\,T}) + \alpha_q (\lambda_q - \frac{2}{3}\mu_q) \nabla.\vec{v}_q \bar{I}$$

Here μ_q and λ_q are the shear and bulk viscosity of phase q, $\vec{F}_q$ is an external body force. $\vec{F}_{lift,q}$ is a lift force, $\vec{F}_{vm,q}$ is a virtual mass force, $\vec{R}_{pq}$ is an interaction force between phases, and p is the pressure shared by all phases.

$\vec{v}_q$ is the interphase velocity and I can be defined as follows.

If $\dot{m}_{pq} > 0$ (i.e., phase p mass is being transferred to phase q), $\vec{v}_{pq} = \vec{v}_p$;
If $\dot{m}_{pq} < 0$ (i.e., phase q mass is being transferred to phase p), $\vec{v}_{pq} = \vec{v}_q$;
$\vec{v}_{pq} = \vec{v}_{qp}$

The above equation must be closed with appropriate expressions for the interphase force $\vec{R}_{pq}$. This force depends on the friction, pressure, cohesion, and other effects, and is subject to the conditions that

$\vec{R}_{pq} = -\vec{R}_{qp}$ and $\vec{R}_{qq} = 0$

FLUENT uses the following form:

$$\sum_{p=1}^{n} \vec{R}_{pq} = \sum_{p=1}^{n} K_{pq} (\vec{v}_p - \vec{v}_q)$$

Where $K_{pq} = K_{qp}$ is the interphase momentum exchange coefficient.

TURBULENCE MODEL

In order to account for the effects of turbulent fluctuations of velocities the number of terms to be modeled in the momentum equations in multiphase is large and this makes the modeling of turbulence in multiphase simulations extremely complex. The turbulence model used for the current simulations is based on Mixture Turbulence Model (MTM). The κ and ε equations describing this model are as follows:

$$\frac{\partial}{\partial t}(\rho_m \kappa)+\nabla.(\rho_m \vec{v}_m \kappa)=\nabla.\left(\frac{\mu_{t,m}}{\sigma_\kappa}\nabla\kappa\right)+G_{\kappa,m}-\rho_m\varepsilon$$

and

$$\frac{\partial}{\partial t}(\rho_m \varepsilon)+\nabla.(\rho_m \vec{v}_m \varepsilon)=\nabla.\left(\frac{\mu_{t,m}}{\sigma_\varepsilon}\nabla\varepsilon\right)+\frac{\varepsilon}{\kappa}(C_{1\varepsilon}G_{\kappa,m}-C_{2\varepsilon}\rho_m\varepsilon)$$

Where the mixture density and velocity, ρ_m and $\vec{v}_m$, are computed from:

$$\rho_m=\sum_{i=1}^{N}\alpha_i\rho_i$$

$$\vec{v}_m=\frac{\sum_{i=1}^{N}\alpha_i\rho_i\vec{v}_i}{\sum_{i=1}^{N}\alpha_i\rho_i}$$

The turbulent viscosity, $\mu_{t,m}$, is computed from:

$$\mu_{t,m}=\rho_m C_\mu\frac{\kappa^2}{\varepsilon}$$

and the production of turbulence kinetic energy, $G_{k,m}$, is computed from

$$G_{\kappa,m}=\mu_{t,m}(\nabla\vec{v}_m+(\nabla\vec{v}_m)^T):\nabla\vec{v}_m$$

BOUNDARY CONDITIONS

At the inlet, all velocities and volume fractions of both phases are specified. The pressure is not specified at the inlet because of the incompressible gas phase assumption (relatively low pressure drop system). The initial velocity of gas and solid phase is being specified as mentioned in Table 1.

The meshing was done using Gambit 1.2. Fine meshing was done for riser inlet and exit sections in order to analyze them in a better way. Under relaxation factors were tuned to achieve convergence. The convergence tolerance was set at 0.001.

The main parameters of the flow inside the system are calculated using an iteration calculation procedure performed by FLUENT. An iterative cycle starts with the introduction of the initial data and/or initial guessed values, boundary conditions, physical conditions and constants. In a second step the program calculate the velocity field from the momentum equation. Then, the mass balance equations as well as the pressure equation are solved.

The next step is to update again the values of the parameters for both phases. The final step is to check on convergence which criterion is fixed by the user. If the convergence criterion is achieved the simulation will stop and give the final results of the system. If not, certain correction values are used to adjust the calculated values and the calculation will start all over again, using as initial data these last corrected values of each parameter.

The coefficient of restitution quantifies the elasticity of particle collisions. It has a value of 1 for fully elastic collisions and 0 for fully inelastic collisions. It is utilized to account for the loss of energy due to collision of particles, which is not considered in the classical kinetic theory. The restitution coefficient is close to unity. In this study, a particle-particle restitution coefficient of 0.95, and a particle-wall restitution coefficient of 0.9 were used.

RESULTS AND DISCUSSIONS ON EXPERIMENTAL WORK

The pressure measurement for the CFB loop was done using the multi tube manometer. All the pressure taps fed to multi tube manometer tubes. The pressure tap through the riser wall had a copper tube inserted into it. Typical arrangement for the pressure measuring system is shown in Figure 5.

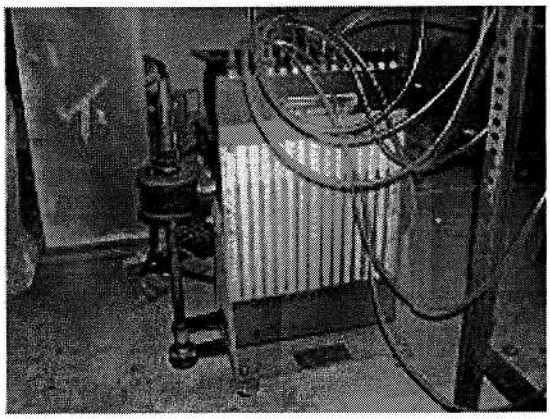

Figure 5: Pressure measurement using multitube manometer

The axial profile for particle distribution in a CFB riser is typically composed of five sections: the acceleration, developed bottom-dense, transition, top-dilute and exit sections. Usually, the acceleration and developed bottom-dense sections are together termed the bottom-dense (lower dense) section.

In the studies of the axial particle distribution, many authors [10, 11,12, 13,14,15,16] have assumed that the pressure gradient at an axial position is proportional to the amount of solid at that position.

Commonly used names for the region of large solids volume fraction are dense region, bottom bed and choked bed. The transition zone is frequently referred to as the acceleration, splash or developing flow region. The region of low solids volume fraction is known as the dilute, transport or fully developed flow region. It is being shown in Figure 6 .

The experimental observation had led to the understanding that the riser flow is generally characterized by: (i) an nonlinear, axial solids volume fraction profile, (ii) upward solids motion in the core of the riser and downward motion along the walls (Core/Annulus, or C/A flow), and (iii) a tendency of solids to form clusters.

Park [17] suggests a new hydrodynamic mode; to represent the gas flow in the dense phase of fluidized Group A powders. The model views that the particles form clusters under the influence of inter-particle forces, giving rise to the formation of a heterogeneous void structure consisting of clusters of particles and interstitial cavities.

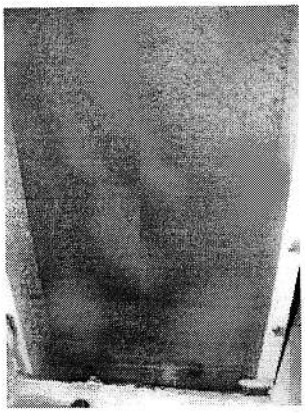

Figure 6: Fluidization behaviour for 600 μm palm shell waste particles.

The experimental results, suggest that riser flow is characterized by continuous formation and disintegration of clusters, and that clusters come in a variety of shapes, sizes, velocities and solids volume fractions. In the acceleration and dilute region, the number and size of clusters appear to increase towards the wall and be maximum near corners. Core clusters may move upwards or downwards, whereas wall clusters generally move downwards. The number of clusters decreases with increasing elevation, especially near the centre of the cross-section. The cluster size near the wall decreases with increasing elevation. Fluidization behaviour for the 1180 μm palm shell powder is being shown in Figure 7.

Figure 7: Fluidization behaviour for 1180 μm palm shell waste particles

Visual observations by of the flow in the riser exit, suggest dunes of significant size in the riser exit connector. It appears that solids in the horizontal connector may settle under gravity, which

means that the remainder of the suspension is accelerated. Acceleration leads to a higher solids velocity in the cyclone and improves its efficiency Similar findings have also been reported by [18].

Although the distinction between `solids turbulence' and `gas turbulence' may be primarily of interest to simulations, it seems reasonable to conclude that full understanding of fast fluidization cannot be obtained without considering turbulence. It seems likely that an interaction between collisions and turbulence is responsible for the macroscopic flow pattern.

An interaction between turbulence and collisions seems consistent with observations of a continuous formation and disintegration of clusters. Clusters may uphold a degree of stability against turbulence and collisions, because they experience less drag than individual particles. In addition, reduced drag increases the slip velocity and allows clusters to collect particles and grow in size.

RESULTS AND DISSCUSSIONS ON NUMERICAL SIMULATIONS

Riser exits can affect the gross behaviour of a CFB. If more solids accumulate near the riser exit then fewer solids reside in the return leg. The lower rate of solids circulation may cause the solids volume fraction in the riser and connector to be lower. However, if the solids accumulation near the riser exit extends into these components, the solids volume fraction may be larger.

Inward/outward motion, secondary flows of the first kind, tangential acceleration/deceleration, and cavity formation near riser exits is mechanisms can account for asymmetric flow in the exit region.

A right angle exit with internal baffle and a blind T riser exits show that the solids volume fraction is more or less constant in the lower half of the riser. In the upper half, a strong increase of solids volume fraction with elevation was observed for the blind T exit, whereas a decrease is found for the right angle exit with the internal baffle. The size and shape of the upstream exit region is strongly dependent on the design of the riser exit. This is being shown in Figure 8.

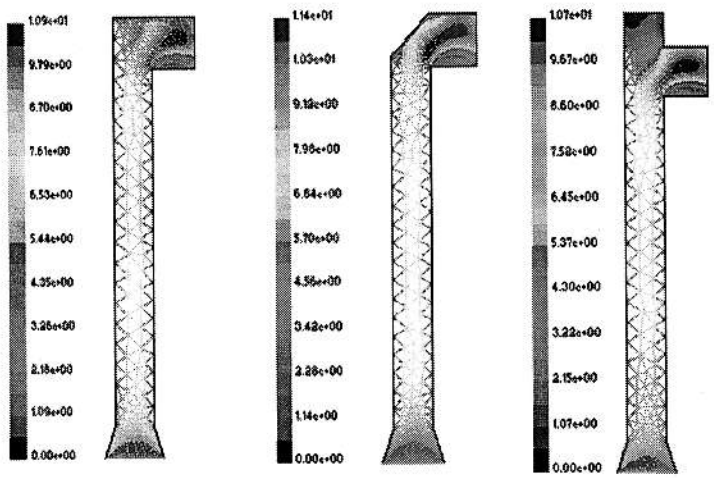

Figure 8: Contours of velocity using volume fraction of air

The right angle exit accumulated more solids than the long radius bend exit. The blind T exit accumulated more solids than the right angle exit, and yielded a higher solids volume fraction in the riser. The solids hold-up is greater for the exit with baffle. The blind T exits shows larger solids volume fractions along the entire riser height, and an increase of solids volume fraction with elevation in the upper half of the riser. This is being shown in Figure 9. The effect of an increase in H_e appeared to be small.

The solids volume fraction remains constant near the exit with internal baffle, but show an increase with elevation in the upper half of the riser for the right angle exit and blind T exit.

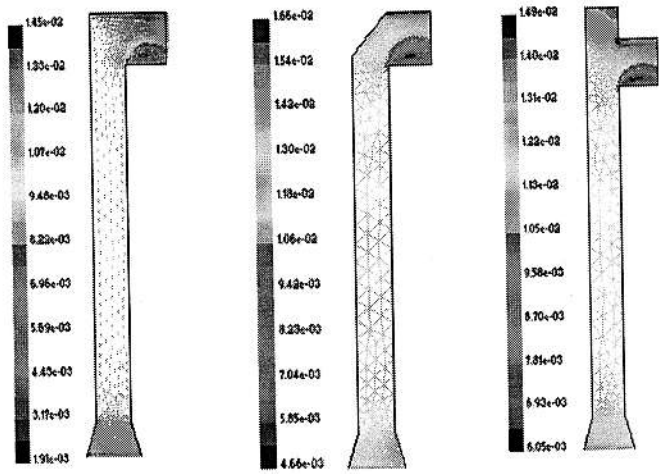

Figure 9: Contours of velocity by volume raction of solid particles

The disengagement exit and the exit with internal baffle invoke an upstream exit region of reduced solids volume fraction. This bend exit yields little or no upstream exit region. The right angle exit, blind T exit and exits with inlet or outlet baffle cause an upstream exit region of increased solids volume fraction as shown in Figure 10. Larger blind T extension heights may invoke a greater upstream exit region, as long as they remain below a critical extension height. Medium size inlet or outlet baffles may yield greater upstream exit regions than large or small baffles.

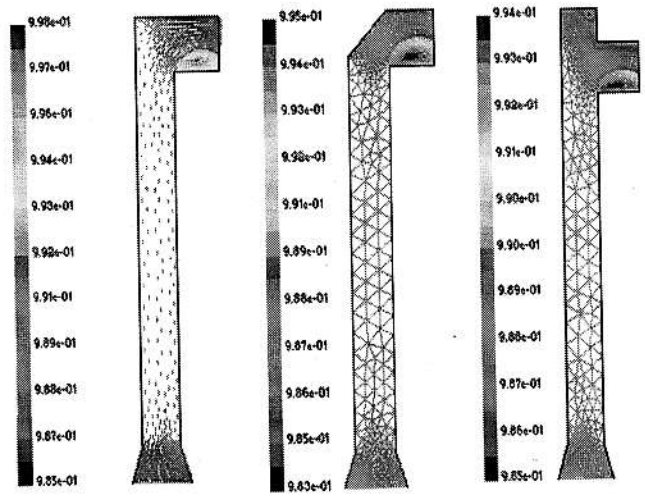

Figure 10: Contours of velocity by volume raction of air

Referring to the Figure 4, which shows a particle in the middle of a bend exit, which experiences a radial acceleration ($\bar{u}_{st}^2/R$) equal to the radial component of the acceleration due to gravity (g cos45° or g /$\sqrt{2}$), i.e. $\bar{u}_{st}^2/R = g/\sqrt{2}$. This condition suggests that radial slip is minimized around $Fr_R = 1/\sqrt{2}$. Larger values of Fr_R may yield more movement of solids to the outside of the riser exit ('outward' movement), and smaller Froude numbers more movement to the inside of the riser exit (`inward' movement). This is being shown in Figure 11.

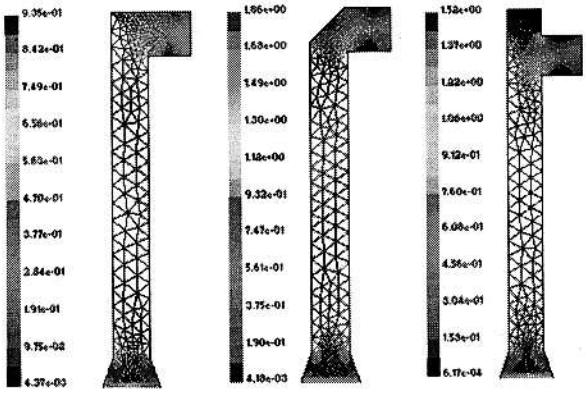

Figure 11: Contours of slip velocity

A radial acceleration balance suggests that inward/outward movement of solids in a riser exit is minimized around a Froude number $Fr_R = 1/\sqrt{2}$. Larger values of Fr_R yield more movement to the outside of the riser exit and smaller values more movement to the inside of the riser exit. From Figure 6 we can see that average exit velocity in the right angle exit bend is about 10 m/s which results in Fr_R much above the $1/\sqrt{2}$. So the predominant movement of the particles is outside of the riser exit. The same trend is also visible for other exits. However, the right angle exit with baffle show more pronounced movement outside the riser exit. It looks that Blind T has little effect of the extension height as compared to right angle exit. Figure 11 suggests that the slip is more prominent in the exit bends. The slip distribution in the various exits are different with right angle exit and with baffle showing greater slip than blind T exit.

CONCLUSIONS

All the above investigations suggest that riser exits can reduce solids hold-up in the riser and yield a region upstream where the solids volume fraction decreases with elevation. Riser exits yield an apparently unaffected solids volume fraction profile or increased solids hold-up and invoke a region where the solids volume fraction increases with elevation. This is evident also from experimental observations.

This suggests an upstream exit region to be defined as the region upstream of the riser exit where flow properties are affected by the riser exit. Similarly, a downstream exit region can be defined as the region downstream of the riser exit where flow properties are affected by the riser exit. The (overall) exit region is the region of the CFB where flow properties are affected by the riser exit, and comprises the upstream exit region, downstream exit region and the riser exit itself.

The results suggest that (i) the right angle exit and the right angle exit with internal baffle invoke an upstream exit region of reduced solids volume fraction, (ii) the bend exit yields little or no upstream exit region, and (iii) the right angle exit, blind T exit and exits with inlet or outlet baffle cause an upstream exit region of increased solids volume fraction.

The upstream exit region is generally characterized by a Core/Annulus structure, but that the solids mass flux profile may be asymmetric. Some riser exits appear to invoke regions near the riser wall where solids motion is upwards.

ACKNOWLEDGEMENT

The authors would like to thank Malaysian Government Commonwealth Secretariat, Public Service Department Malaysia, Putrajaya for funding the PhD program. Thanks are also due to Universiti Teknologi Malaysia for providing financial supports for developing and building the CFB test facility in the Department of Mechanical Engineering, UTM, Skudai, Johor, Malaysia.

REFERENCES

[1] Gilbertson, M.A. and Yates, J.G. (1996). The Motion of Particles Near a Bubble in a Gas-Fluidized Bed. *Journal of Fluid Mechanics* 323: 377-385

[2] Pain, C.C., Mansoorzadeh, S. & de Oliveira, C.R.E. (2001). A Study of Bubbling and Slugging Fluidized Beds Using the Two-Fluid Granular Temperature Model. *International Journal of Multiphase Flow* 27, 527-551.

[3] Taghipour, F., Ellis, N. & Clayton, W. (2003). CFD Modeling of a two-dimensional Fluidized Bed Reactor, University of British Columbia.

[4] Jalil R., Tasirin S. & M. S. Takriff (2002). [4]Computational Fluid Dynamics (CFD) in Fluidized Bed column: effect of Internal Baffles, The proceedings of RSCE Oct 2002, Malaysia.

[5] Hansen, K. G., Madsen, J., Ibsen, C. H., Solberg T. & Hjertager B. H. (2002). An experimental and computational study of a gas-particle flow in a scaled circulating fluidized bed. *World Congress on Particle Technology, Sydney, NW, Australia.*

[6] Arastoopour, H., Benyahia, S., Knowlton, T. M. & Massah H. (2004) Simulation of particle and gas flow behavior in the riser section of a circulating fluidized bed using kinetic theory approach for the particulate phase. *Powder Technology (Articles in Press).*

[7] Fluent 6.1, (2001). User's guide. Fluent Incorporated.

[8] Weinstein, H, H.J. Feindt, L. Chen, R.A. Graff (1992). The measurement of turbulence quantities in a high velocity fluidized bed. *Proceedings of 7th International Conference on Fluidization,* O.E. Potter, D.J. Nicklin (eds), Engineering Foundation, NY, 305 - 312.

[9] Wu, S, M. Alliston (1993). Cold model testing of the effects of air proportions and reactor outlet geometry on solids behaviour in a CFB, Proceedings of 12th International Conference on Fluidized Bed Combustion, L.N. Rubow, G. Commonwealth (Eds.), ASME, 1003 - 1009.

[10] Xu, G. and Shiqiu, G. Necessary parameters for specifying the hydrodynamics of circulating fluidized bed risers – a review and reiteration. Powder Technology 137, 63-76, 2003.

[11] Davidson, J.F. Circulating Fluidized bed hydrodynamics. Chemical Engineering Science 113, 249-260, 2000.

[12] Contractor, R., Dry R.J., White C., Mao Q.M., Konstantinidis S. and Potter O. E. Circulating fluidized beds-diameter, solid hold up, axial gas mixing and contact efficiency. Powder Technology 111: 132-144, 2000.

[13] Mandal, S., D. K. Acharjee and P. S. Gupta. Distribution of Axial Voidage in the riser of a Circulating Bed. Indian Journal of Chemical Technology, Vol. 2, January 1995.

[14] Weinstein, H., L. Chen, and A. Kostazos. The Radial Pressure Gradient in a Fluidized Beds Risers. Fluidization and Fluid-Particle Systems, AIChE Annual Meeting, 1995.

[15] Van der Ham, A. G. J., W. Prins and W. P. M. van Swaaij. Hydrodynamics of a Pilot Plant Scale Regularly Packed Circulating Fluidized Bed. Fluid-Particle Processes: Fundamentals and Applications, AIChE Symposium Series, 1993.

[16] Yerushalmi, J. An Overview of Commercial Circulating Fluidized Bed Boilers. Circulating Fluidized Bed Technology II, 1985.

[17] Park, J.Y. The clustered dense phase models for group A fluidization: Dense phase hydrodynamics. Chemical Engineering Science, Vol. 58: 193-202, 2003.

[18] Muschelknautz, E, U. Muschelknautz. Special design of short entrance ducts to recirculating cyclones. Proc. 5th Int. Conf. Circ. Fl. Bed, preprint volume, Eq6 1 –6, 1996.